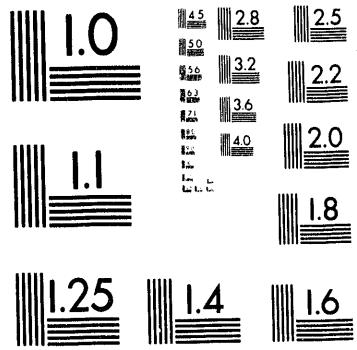
1.0
1.1
1.25
1.4
1.6
1.8
2.0
2.2
2.5
2.8
3.2
3.6
4.0
4.5
5.0
5.6
6.3
7.1

1 of 1

CONF-9309128--14

PNL-SA-22183

POSTIRRADIATION EXAMINATION OF BEATRIX-II, PHASE I

O. D. Slagle
T. Takahashi[a]
F. D. Hobbs
K. Noda[a]
D. L. Baldwin
G. W. Hollenberg
R. A. Verrall[b]

September - October 1993

Presented at the
6th International Conference
on Fusion Reactor Material
September 27 - October 1, 1993
Stressa, Italy

Work supported by
the U.S. Department of Energy
under Contract DE-AC06-76RLO 1830

Pacific Northwest Laboratory
Richland, Washington 99352

(a) Japan Atomic Energy Research Institute
Tokai-mura, Ibaraki-Ken
(b) AECL Research, Chalk River Laboratories
Chalk River, Ontario, Canada

POSTIRRADIATION EXAMINATION OF BEATRIX-II, PHASE I

O. D. Slagle[1], T. Takahashi[2], F. D. Hobbs[1], K. Noda[2], D. L. Baldwin[1], G. W. Hollenberg[1] and R. A. Verrall[3]

[1] Pacific Northwest Laboratory[(a)], Richland, Wash. USA
[2] Japan Atomic Energy Research Institute, Tokai-mura, Ibaraki-Ken, Japan
[3] AECL Research, Chalk River Laboratories, Chalk River, Ontario, Canada

ABSTRACT

BEATRIX-II is an in situ tritium recovery experiment that was designed to characterize the behavior of lithium ceramics irradiated to high burnup in a fast neutron flux. Postirradiation examination was carried out on the Phase I vented canisters: one containing a Li_2O ring capable of temperature changes and the other a Li_2O solid specimen with a center temperature of 1000°C.

The tritium inventory of the ring specimen at 650°C was determined to be in the range from 0.2-0.6 wppm while for the solid specimen the inventory varied from 1.4 wppm at the surface to 0.06 wppm at the inner surface. Downstream transport of the Li_2O by the sweep gas was determined to be insignificant from analyses of acid rinses of selected canister surfaces. Densification and restructuring of the solid specimen during irradiation resulted in the development of a central annulus. Ceramography was used to characterize the columnar grain structure and the mechanisms involved in its evolution.

(a) Pacific Northwest Laboratory is operated for the U. S. Department of Energy by Battelle Memorial Institute under Contract DE-AC06-76RLO 1830.

INTRODUCTION

BEATRIX-II is an IEA sponsored experiment with emphasis on tritium recovery from lithium ceramic materials irradiated in a fast neutron reactor(FFTF) that simulates the environment of a fusion blanket. The participants are Japan, Canada and the U.S. The in situ tritium recovery experiments provided data on the performance of Li_2O and Li_2ZrO_3 under irradiation conditions covering a range of sweep gas compositions and temperatures. The experiment consisted of two separate irradiation cycles which included two vented tritium recovery canisters each. Phase I started in January 1990 and operated for 300 Effective Full Power Days (EFPD) while Phase II started in May 1991 and operated for 200 EFPD of irradiation. Both Phase I and II resulted in lithium burnups of 5%. In addition to the vented canisters, BEATRIX-II also included nonvented canisters to provide data on irradiation damage in Li_2O single crystals and the compatibility of lithium ceramics and beryllium in a fast neutron environment.

Postirradiation examination of the irradiated lithium ceramics is being carried out to evaluate their physical and chemical stability during irradiation and to determine the final tritium inventory. This final inventory establishes a baseline for determining the tritium inventory for various testing temperatures and sweep gas compositions. This paper presents the results of the postirradiation examination of the Phase I vented-canister Li_2O specimens. The results of a spectroscopic study of the Li_2O single crystals irradiated in Phase I are presented in another paper in these proceedings[1]. Postirradiation examination of the Phase II, Li_2O and Li_2ZrO_3 vented canisters is underway.

BACKGROUND

The design and operation of the BEATRIX-II, Phase I in situ tritium recovery experiment has been described previously [2-5]. Phase I of the experiment involved two Li_2O specimens with initial ^6Li enrichments of 61 at% irradiated to lithium burnup exceeding 4%. The ring specimen capable of temperature changes was 1.85 cm in diameter with a wall thickness of 1.5 mm and operated in the temperature range from 510 to 650°C. The temperature-gradient solid specimen was 1.75 cm in diameter with a range of temperatures from 430 to 1000°C.

The chemical and physical integrity of the specimen is expected to be influenced by the temperature and sweep gas compositions under which the material operated. In addition to temperature changes during startup/shutdown the ring specimen was subjected to a number of temperature transients on the order of 50 or 100°C which were incurred over times less than 15 seconds. The primary sweep gas used in the experiment was He-0.1% H_2 but helium and He-0.01% H_2 and He-1.0% H_2 were also used at times to evaluate the effect of hydrogen content on the tritium recovery behavior.

The experiment was terminated by a controlled "scram" or rapid decrease in reactor power. The reactor shut down occurred over 2 minutes time and is expected to have contributed on the order of a minute of generation rate to the tritium inventory of the specimens or 0.02 wppm. However, the

microstructures of the specimens are expected to have changed very little during shut down.

EXPERIMENTAL RESULTS

Neutron Radiography

After removal from the irradiation test vehicle and prior to disassembly, the two vented canisters were neutron radiographed. The radiographs indicated that both specimens were intact and that the initial specimen geometry had been maintained throughout the experiment. The ring specimen was observed to contain a number of cracks which could have occurred during the startup/shutdown thermal transients. In spite of the cracking, the cylindrical geometry and positioning of the ring specimen in the canister was maintained by the inner nickel screen. In the inlet gas plenum, located beneath the ring specimen, a region of neutron absorbing residue was found which appeared to be Li_2O. This residue will be discussed later. Because of the large diameter of the solid specimen, only the outer edges of the specimen were resolvable. The downstream boundary/edge of the solid specimen was intact and there appeared to be no discernable downstream transport of the specimen by the sweep gas.

Capsule Disassembly

The capsules were disassembled by slitting the outer canister lengthwise so that the cladding could be separated. The ring specimen was found to be fragmented into pieces of a nominal size of one cm^2. There was no particular crack pattern. The eleven individual pellets in the solid specimen stack had interdiffused during irradiation and the interfaces between pellets were no longer discernable. The solid specimen was also found to be tightly bonded to the capsule walls and removal of the pellets left a layer of the specimen material on the capsule wall. In general, the solid specimen was fragmented into radial sections although the axial center portion of the specimen was an intact cylinder. This center portion had initially consisted of three solid cylindrical pellets but after irradiation a center void or annulus was found to have been formed throughout this section. This center annulus had a diameter which was in the range of 0.38 to 0.45 cm. For a 1.7 cm diameter pellet, these diameters represent 5-7% of the volume. The center pellets were initially 86, 87 and 92 %TD. It is hypothesized that the center void was a result of additional pellet densification.

The sweep gas plenums on either end of the capsules were found to have a black "shiny" deposit on the surfaces that was thought to be vapor-transported Li_2O. The capsule components were acid-washed and the resulting solutions were found to contain lithium. The total weight of the deposit in the top and bottom gas plenums of the solid specimen was equivalent to 1.0×10^{-4}% and 0.4×10^{-4}% of the total specimen weight for the top and bottom, respectively. Thus the material transported out of the solid specimen region by the sweep gas was only a negligible percentage of the total specimen weight. For the ring specimen the equivalent weight of the deposit was the same for both the top and the bottom: 3.5×10^{-4}% of the total sample weight. The amount of material found in the bottom end cap or inlet gas plenum of the ring specimen was much smaller than expected based on the extent of the dark area seen in the neutron radiograph. During disassembly a black powder was observed to fall from the capsule. Unfortunately it was not possible to capture and

quantify the amount of this material. This observation suggests that the residue seen in the radiograph was material which had physically fallen off the inner wall of the ring specimen and collected in the lower plenum area as opposed to vapor-deposited material.

Microstructural Characterization

On a macroscopic scale the postirradiation condition of the ring specimen was not noticeably different from the preirradiation condition. The thickness of the ring was found to have increased approximately 10% from its original thickness of 1.5 mm. The associated density decrease from the initial density of 80% TD was also evident in the scanning electron microscopy observations of the pre- and postirradiation specimens. The grain size of the material remained essentially constant at 5 μm.

The irradiated solid specimen was significantly different from the pre-irradiated specimen. In addition to the formation of a center annulus in the initially solid pellets, the occurrence of a large grain microstructure was visually apparent. An intact pellet from a location just below the center of the solid specimen was chosen for ceramography. This pellet had an initial density of 85% TD and developed a 0.45 cm diameter center annulus during irradiation. The resulting composite photomicrograph is shown in Figure 1. The microstructure of the solid specimen shown in Figure 1 exhibits classic columnar grain growth in a temperature gradient and is very similar to microstructures observed in fast reactor fuel elements[6]. This microstructure is characterized by a succession of regions starting at the outer surface: 1. as fabricated structure with grain sizes in the range of 25-40μm; 2. equiaxed grain region with grains on the order of 100μm; 3. Columnar grain regions with grains sizes on the order of 200μm wide and 1500μm long. The formation of this type of microstructure in fission type fuels has been attributed to the formation and migration of lenticular pores up a steep temperature gradient. The equiaxed region is characterized by the formation of larger grains and lenticular shaped pores which are oriented perpendicular to the radius or thermal gradient. As the temperature increases these lenticular pores become sufficiently mobile to migrate up the temperature gradient. This pore migration sweeps out porosity in the path of the lenticular pore and enlarges the grain behind it, leading to the formation of large columnar grains parallel to the radius. In the columnar grain region of Figure 1, lenticular pores can be found at the high temperature end of the columnar grains. In fast reactor fuels the formation and movement of the lenticular shaped pores has been attributed a vapor-transport mechanism from the hot to cold side of the pore. The obvious similarity of the microstructure of the postirradiated BEATRIX-II solid specimen to fast reactor fuel provides strong evidence that the migration of the lenticular pores up the thermal gradient by a vapor-transport method plays a major role in the formation of the columnar grains in the BEATRIX-II solid specimen. This migration of the pores to the center of the solid specimen during irradiation also contributes to the formation of a center annulus.

Tritium Inventory

Measurements of the retained tritium in selected sections of the ring and solid specimens were used to characterize the tritium inventory at the time of shutdown. As noted above, the experiment was terminated by a rapid decrease

in reactor power that was expected to limit the increase in the tritium inventory to less than 0.02 wppm.

Measurement of the tritium inventory along the length of the ring specimen was carried out for four different axial locations. The results are given in Table 1. The top and bottom sections represented material within one cm from the end since the selected section contained end surfaces. Upper and lower center are only approximate locations. The analysis was done by melting the selected sections and determining the tritium released using a variation from the method described previously[7]. The present analysis used a gas sweep rather than evacuation for obtaining the gas sample. The measured tritium inventory increased smoothly from the bottom to top of the specimen. The top and bottom of the specimen are different in two aspects: the specimen temperature and the tritium concentration in the sweep gas. Because the specimen is located at the bottom of the reactor, the neutron flux decreases from top to bottom so that the top of the specimen is expected to be as much as 30°C hotter than the bottom. However, inreactor observations[2-4] have indicated that higher temperatures result in a lower tritium inventory which is contrary to the results in Table 1. Alternatively, the sweep gas flow is from the bottom to the top so that at the top of the specimen the sweep gas contains a higher partial pressure of HTO/HT. This higher partial pressure would tend to decrease the tritium recovery rate and therefore is one possible explanation for the increase in tritium inventory with axial position.

The radial variation of the tritium inventory in the solid specimen was determined by radially sectioning the specimen into five sections and determining the tritium retention by melting as above[6]. The pellet chosen for this analysis was the same one used in the microstructure characterization(Figure 1). The measured tritium inventories are listed in Table 2 along with the outer and inner radii of the section analyzed. Calculated temperatures were determined by proportionally increasing the original calculated radial thermal profile for the preirradiated specimen to fit the thermocouple measurements for the inner radius of the specimen. Measured centerline temperatures varied from 950 to 1030 C compared to a calculated temperature at the radius of the center annulus of 910°C. The temperature at the center annulus was chosen to be 1000°C.

Although there is considerable uncertainty in the radial position and the corresponding temperature, the data in Table 2 clearly indicate that the tritium inventory decreases rapidly as the temperature increases and appears to reach a minimum at sample #2 before increasing slightly as the temperature increases. This type behavior has been predicted by Billone et al[8]. The decrease in inventory with increasing temperature in the outer regions of the specimen is associated diffusional/desorption release mechanisms while the increase in inventory at the higher temperature is associated with an increased solubility of tritium in Li_2O.

Axial measurement of the tritium retained in the outer surface of the solid specimen was carried out by dissolving four different axial segments of the material adhered to the cladding during disassembly. The resulting solutions were analyzed for tritium and lithium to determine the tritium inventories which ranged from 0.7 to 1.4 wppm. There was no consistent trend of the data with axial positon and the range in data is consistent with the expected uncertainties in the measurement procedures. From the identifiable

uncertainties in the data, the measured inventories are expected to represent lower limits on the tritium inventory in the outer region of the solid specimen. It was thought that the tritium inventory would increase at the outer edge of the specimen as a result of the lower temperature; however, because of the uncertainties, the radial dependence of the inventory near the outer edge of the solid specimen remains undefined.

DISCUSSION

A comparison of the tritium inventories for the ring and solid specimen requires information on inventories at the same temperature. Because of the extensive database available for the operation of the ring specimen, it is possible to develop an empirical temperature relationship for the inventory of ring specimen. The tritium inventory has an inverse relationship to the controlling mechanisms for tritium release which are typically lattice/grain boundary diffusion and adsorption/desorption processes at the surface[9,10]. These release mechanisms are controlled by one or more processes with Arrhenius type temperature dependencies. As a first approximation the inventory (I) will be described by an inverse Arrhenius temperature (T) dependence:

$$(1/I) = (1/I_o) \exp(-Q/RT) \qquad (1)$$

Evaluation of I_o and the effective activation energy (Q) was carried out by analyzing a series of temperature transients carried out on the ring specimen just prior to shutdown. The temperature change series of 630-530-630°C was used to determine an inventory change of 0.43 wppm for the temperature change of 530 to 630°C. This inventory change together with the average of the inventories in Table 1 was used to determine $I_o = 5.6 \times 10^{-4}$ wppm and Q = 48 kJ/mol.

The empirical relationship for the inventory (Eqn 1) was used to calculate tritium inventories at the respective solid specimen temperatures listed in Table 2. For the solid specimen sample #1, the range of the predicted ring specimen inventories includes the measured inventory. The remaining four samples of the solid specimen had inventories that are much lower than predicted by the extrapolation of the ring specimen inventory. The reason for this large discrepancy may be related to the difference in microstructure between the ring and the inner regions of the solid. By comparing the radial position in the solid specimen listed in Table 2 with the microstructure in Figure 1, we find that sample #1 is located in the as-fabricated region, sample #2 is located primarily in the equiaxed grain region and samples 3-5 are in the columnar grain region. It appears as if the low tritium inventories are be associated with the large grain size and high density of the restructured region of the solid specimen.

Comparison of the final tritium inventory (0.2-0.6 wppm) for the ring specimen with similar experiments on Li_2O is complicated because of the many variables which affect the final inventory. The shutdown conditions for BEATRIX-II were an average specimen temperature of 630°C and a helium sweep gas with 0.1% H_2. Lower temperatures and lower hydrogen concentrations in the sweep gas were found to result in higher inventories[2-5]. CRITIC-I[11] had final average inventories of 1 wppm for a temperature of 600°C and a final sweep gas of He-0.01% H_2. Both the lower temperature and lower hydrogen concentration

favor the slightly higher inventory. The VOM experiment on Li_2O pellets[12] had final inventories in the range of 0.5-0.9 wppm after operation at 740°C in a helium sweep gas. The higher temperature favors a lower inventory, but this could easily be offset by the higher inventory expected for a helium sweep gas. This comparison suggests that, within the expected range of experimental parameters, the final inventories of these three experiments are in agreement.

CONCLUSIONS

Operation of the BEATRIX-II experiment provided an extensive data base on the tritium recovery from Li_2O in a fast neutron environment. The Li_2O in Phase I of the experiment was irradiated to lithium burnups in excess of 4% while operating at temperatures from 400 to 1000°C in helium sweep gases with additions of 0 to 0.1%H_2. Postirradiation examination of the specimens indicated that the material underwent extensive microstructural changes but remained physically intact while efficiently releasing the generated tritium to maintain a low tritium inventory. Lithium transport out of the specimen area was negligible. Based on these results, it is concluded that Li_2O should be considered as one of the leading candidates for use in a solid breeder fusion blanket application.

REFERENCES

1. N. Masaki, K. Noda, H. Watanabe, R. G. Clemmer and G. W. Hollenberg, presented at the 6th Int Conf on Fusion Reactor Materials (ICRFM-6), Stresa, Lago Maggiore, Italy, 1993

2. G. W. Hollenberg, H. Watanabe, I. J. Hastings, and S. E. Berk. **J Nucl Mater 191-194**, 23-29 (1992)

3. T. Kurasawa, O. D. Slagle, G. W. Hollenberg, and R. A. Verrall. **Fusion Technology 19**, 931-937 (1991).

4. O.D. Slagle, T. Kurasawa, R. A. Verrall, and G. W. Hollenberg. **J Nucl Mater 191-194**, 214-218 (1992).

5. T. Kurasawa, O. D. Slagle, G. W. Hollenberg, and R. A. Verrall. In **Ceramic Transactions**, Vol 27, edited by I. J. Hasting and G. W. Hollenberg, pp 299-314, 1991, The American Ceramic Society, Westerville, Ohio.

6. D. R. Olander, Fundamental Aspects of Nuclear Reactor Fuel Elements, TID-26711-P1, Technical Information Center - Energy Research and Development Administration (1976)

7. D. L. Baldwin and G. W. Hollenberg. **J Nucl Mater 141-143**, 305-310 (1986)

8. M. C. Billone, H. Attaya, and J. P. Kopasz. in Proceeding of the International Workshop on Ceramic Breeder Interactions, October 26-29, 1992, ed M Yamawaki, University of Tokyo, Tokyo, Japan (1993)

9. M. C. Billone, H Attaya, and J. P. Kopasz. ANL/FPP/TM-260, Argonne National Laboratory, Argonne, Ill (1992)

10. G. Federici, A. R. Raffray and M. A. Abdou. **J Nucl Mater 173**, 185-213 (1990)

11. R. A. Verrall, D. H. Rose, J. M. Miller, I. J. Hastings and D. S. MacDonald. **J Nucl Mater 179-181**, 855-858 (1991)

12. T Kurasawa, H. Yoshida, H. Takeshita, H Watanabe, T. Miyauchi, T. Matui, H. Umei, Y. Naruse. **J Nucl Mater 133-134**, 196-200 (1985)

Table 1. Axial distribution of the tritium inventory in the ring specimen

Axial Position	Tritium Inventory(wppm)
Top	0.61
Upper Center	0.44
Lower Center	0.26
Bottom	0.23

Table 2. Radial distribution of the tritium inventory in the solid specimen compared to extrapolated inventories for the ring specimen

Specimen No.	Radial Position (r/r_o)	Temperature Calculated (C°)	Tritium Inventory (wppm)	Predicted Inventory (wppm)
1	0.964-0.916	467-514	1.44	1.49-0.93
2	0.898-0.776	532-649	0.056	0.79-0.31
3	0.758-0.636	665-772	0.063	0.28-0.15
4	0.618-0.496	787-876	0.069	0.14-0.09
5	0.478-0.269	886-1000	0.062	0.09-0.05

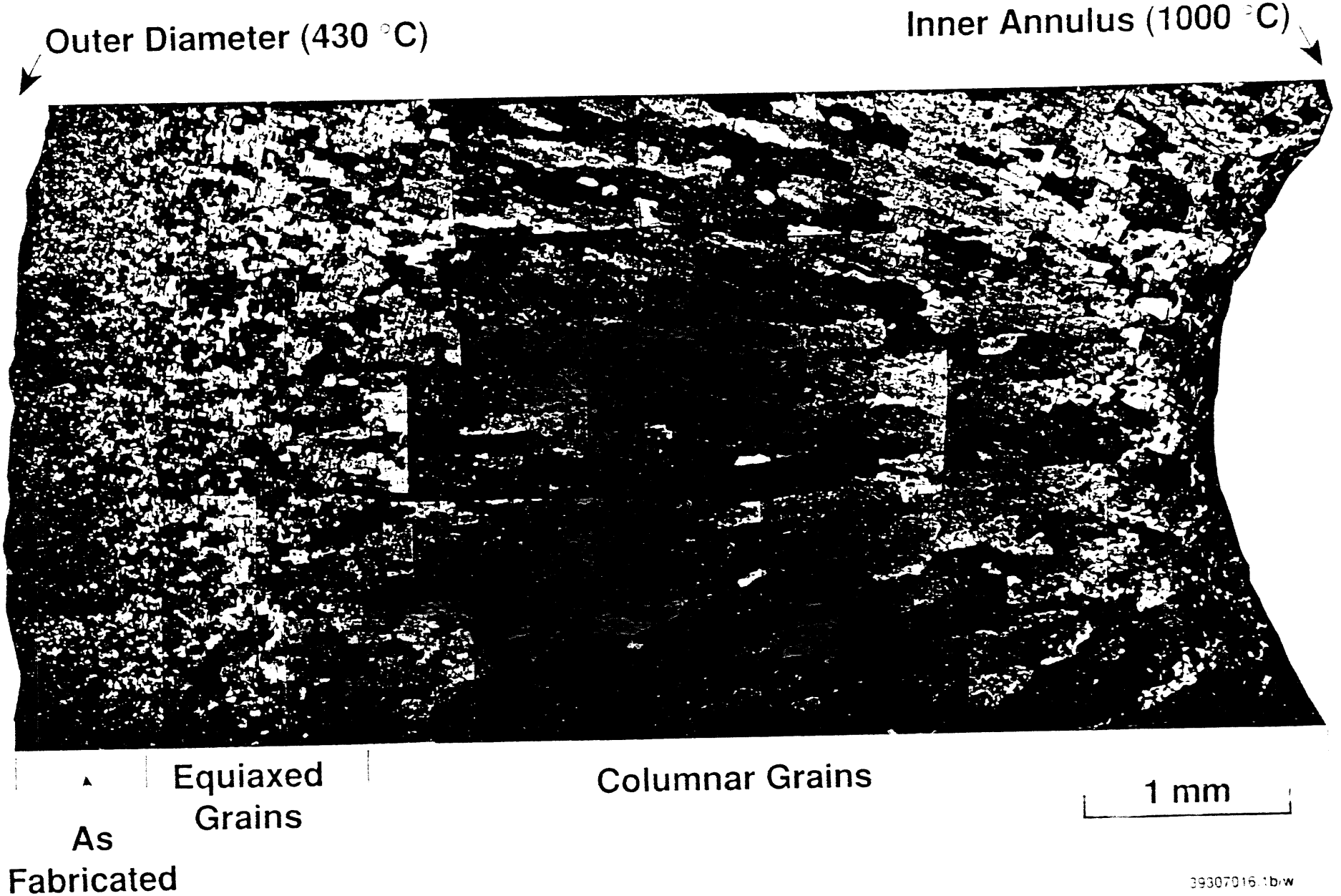

Figure 1. Microstructure of radial cross section of the BEATRIX-II solid specimen

DATE FILMED

1 / 14 / 94

END